

## Study of liquid crystalline order by NMR

*K. V. Ramanathan*

**Abstract** | The liquid crystalline phase represents a unique state of matter where partial order exists on molecular and supra-molecular levels and is responsible for several interesting properties observed in this phase. Hence a detailed study of ordering in liquid crystals is of significant scientific and technological interest. NMR provides several parameters that can be used to obtain information about the liquid crystalline phase. Of these, the measurement of dipolar couplings between nuclei has proved to be a convenient way of obtaining liquid crystalline ordering since the coupling is dependent on the average orientation of the dipolar vector in the magnetic field which also aligns the liquid crystal. However, measurement of the dipolar coupling between a pair of selected nuclei is beset with problems that require special solutions. In this article the use of cross polarization for measuring dipolar couplings in liquid crystals is illustrated. Transient oscillations observed during cross polarization provide the dipolar couplings between essentially isolated nearest neighbor spins which can be extracted for several sites simultaneously by employing two-dimensional NMR techniques. The use of the method for obtaining heteronuclear dipolar couplings and hence the order parameters of liquid crystals is presented. Several modifications to the basic experiment are considered and their utility illustrated. A method for obtaining proton–proton dipolar couplings, by utilizing cross polarization from the dipolar reservoir, is presented. Some applications are also highlighted.

### Introduction

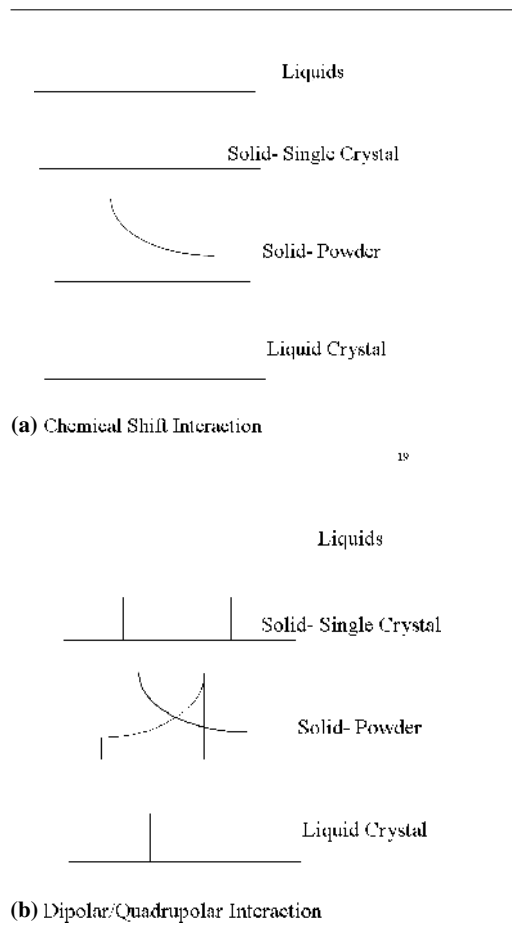
Nuclear magnetic resonance is a powerful technique for the study of molecular structure and dynamics. Over the years it has been exploited extensively for the study of partially ordered systems of which liquid crystalline materials form an important part (1–3). Particularly, for nematic liquid crystals which are easily oriented in the magnetic field required for NMR studies, the spectra provide characteristic shifts or splittings which provide detailed information on ordering and dynamics at every chemical site in a liquid crystalline molecule. Characteristic spectra that are obtained for a nucleus in the liquid crystalline phase under the influence of the chemical shift anisotropy interaction and dipolar or quadrupolar couplings are depicted in

fig. 1. Fig. 1 also provides a comparison of the spectra in the solution phase and in the solid in the single crystal as well as the powder form. In the early years, proton NMR spectroscopy provided limited information (4-5). Due to its inherent limitations for use with ordered systems arising out of strong proton–proton dipolar couplings, its application was limited to small molecules oriented in liquid crystalline matrices (1,2). On the other hand deuterium was found to be a convenient nucleus for the study of liquid crystals and extensive work has subsequently been carried out using  $^2\text{H}$  NMR spectroscopy (6,7). Deuterium has the advantage that it experiences a large quadrupolar interaction while the dipolar coupling between deuterium nuclei is fifty times smaller than that between protons.

*NMR Research Centre,  
Indian Institute of Science,  
Bangalore 560 012, India  
kvr@nrc.iisc.ernet.in*

**Keywords:** NMR; Nematic liquid crystals; Dipolar couplings; Order parameter. Cross-polarisation, Two-Dimensional NMR, SLF

Figure 1: Characteristic spectral patterns observed for a sample in different phases in the presence of (A) chemical shift anisotropy (B) dipolar or first order quadrupolar interactions.



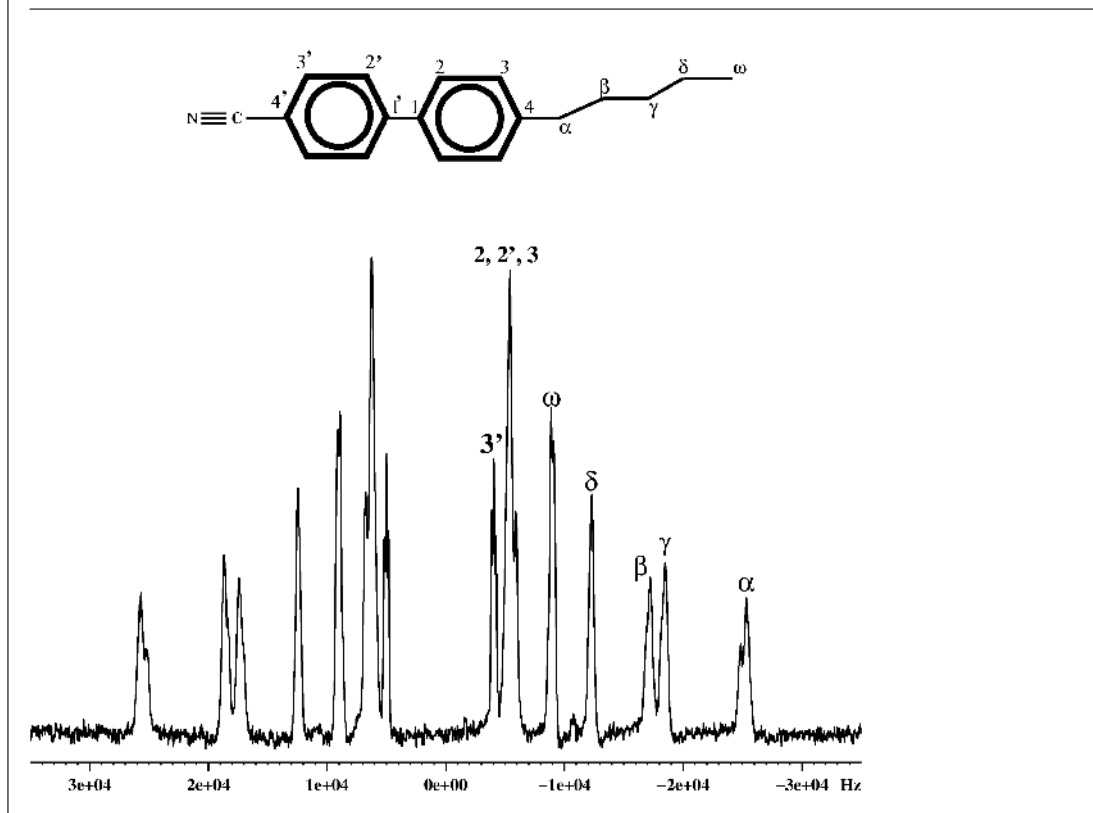
Deuterium turned out to be a convenient nucleus particularly for systems that are easily oriented by a magnetic field such as nematics and a few cases of smectic and cholesteric liquid crystals. Deuterium provided a pair of well separated lines due to the quadrupolar interaction. Since the quadrupolar interaction is modulated by local motion and is partially averaged, each chemical site in the liquid crystal molecule provides a distinct quadrupolar doublet that enables investigation of the molecular dynamics. Fig. 2 shows a typical  $^2\text{H}$  NMR spectrum of an oriented sample of perdeuterated liquid crystal, 4-pentyl-4'-cyanobiphenyl (5CB). The quadrupolar interaction is also dependent on the orientation of the molecule in the magnetic field, which enables investigation of liquid crystalline ordering and director dynamics. However deuterium NMR has the problem of low sensitivity in natural abundance which means that the molecule needs to be either partially or uniformly deuterated. This proved to

be a limitation in view of the cost and difficulties associated with chemical synthesis. The utility of  $^{13}\text{C}$  NMR spectroscopy for studying nematic liquid crystal was first demonstrated by Hohener et al. (8). It was shown that for molecules that are oriented in a magnetic field, proton decoupled natural abundance  $^{13}\text{C}$  NMR spectra provided narrow well resolved lines. Unlike the solution phase, the chemical shift anisotropy in the liquid crystalline phase is only partially averaged. This results in a spectrum in the mesophase which is spread over a much larger frequency range. The change in the chemical shift upon going into the nematic phase from the isotropic phase, reflects the ordering of the liquid crystal molecule in the magnetic field as well as the dynamics along the length of the molecule [9].

Another important parameter that provides useful information on the liquid crystalline phase is the heteronuclear dipolar coupling. One of the first demonstrations of this approach has been made with the study of  $^2\text{H}$ - $^{13}\text{C}$  dipolar couplings in N-(4-methoxy-benzylidene)-4-n-butylaniline (MBBA) deuterated at a specific site [8]. Similar studies have been performed on systems containing  $^{19}\text{F}$  and using  $^{19}\text{F}$ - $^{13}\text{C}$  dipolar couplings [10,11]. However, a more general and attractive approach would be to utilize  $^1\text{H}$ - $^{13}\text{C}$  dipolar couplings. The use of the 2D SLF procedure for this purpose was first carried out in the case of MBBA [8]. The  $^{13}\text{C}$  chemical shifts and the corresponding  $^{13}\text{C}$ - $^1\text{H}$  dipolar splittings were displayed in a 2-dimensional plot along the  $F_2$  and  $F_1$  axes respectively. However, in this method, the presence of the homonuclear dipolar couplings tends to make the lines broad along the  $F_1$  axis. The problem of the elimination of the proton-proton dipolar couplings has been addressed by employing the variable angle sample spinning (VASS) technique [12]. Due to the off-magic angle spinning, the proton dipolar coupling is significantly reduced and further use of the multiple pulse decoupling during the  $t_1$  period enables near elimination of proton dipolar couplings. The  $^{13}\text{C}$ - $^1\text{H}$  dipolar splittings observed along  $F_1$  are to be suitably scaled to include the effect of VASS and the multiple pulse decoupling, to obtain the actual dipolar couplings. This method has been used for the study of a large number of liquid crystalline systems [13]. Modifications to this technique have also been suggested which enable short range [14] and long range [15, 16] dipolar couplings to be measured accurately.

Another approach that can be utilized for the measurement dipolar couplings is the use of transient oscillations observed during cross-polarisation [17,18]. Cross-Polarisation or CP

Figure 2: Deuterium NMR spectrum of a sample of the liquid crystal 5CB spontaneously oriented in the magnetic field.



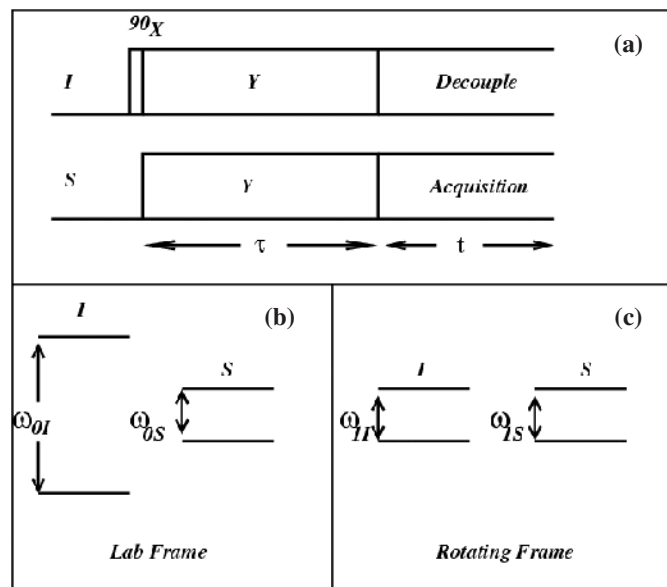
traditionally has been used in solids for enhancing weak signals of nuclei with low gyromagnetic ratio ( $\gamma$ ) and the principle of its working is depicted in fig. 3. Nuclei with a large  $\gamma$ , such as protons, have a large energy level separation in a magnetic field. This gives rise to a significant population difference between the two Zeeman levels of protons due to Boltzmann distribution. Consequently, protons have a large magnetic polarization and give rise to signals of much higher intensity than nuclei with a low  $\gamma$  such as  $^{13}\text{C}$  and  $^{15}\text{N}$ . It is possible to enhance the signal of a low  $\gamma$  nucleus by polarisation transfer from proton provided their energy levels match and a coupling such as the dipolar coupling exists between them. Such a matching of energy levels is not possible with the static  $B_0$  magnetic field, but is possible in the so-called rotating frame with the magnetizations of the two nuclei spin locked to r.f. magnetic fields applied at their respective resonating frequencies, which is known as the Hartmann and Hahn match (19). In fig. 3a, this takes place during the  $\tau$  period when a transfer of polarisation from protons to the low  $\gamma$  nuclei takes place through the dipolar coupling between them, enhancing the signal of the latter. In solids with a strong dipolar coupling network, CP has mainly been used for

enhancing the signals of low  $\gamma$  nuclei. However in the case of essentially isolated pair of nuclei, polarisation transfer between nuclei takes place in a coherent and oscillatory fashion and the first use of such CP oscillations for measuring dipolar couplings and studying liquid crystalline order was carried out at the Indian Institute of Science [20]. Two-dimensional NMR methods incorporating the CP contact period as the evolution period have been developed. Several modifications to the standard cross-polarisation pulse scheme have also been suggested [21–26] in order to enhance the efficiency of the method. A method that does not require Hartmann-Hahn match and hence minimize the use of r.f. power has been proposed and its utility demonstrated [27,28]. A method for indirectly monitoring proton dipolar couplings using the carbon chemical shift dispersion has also been suggested [29]. These are described in more detail in the following sections. Some of the pulse schemes that have been utilized are shown in Fig. 4.

### Measurement of Dipolar Couplings from Cross-Polarisation

Observation of dipolar oscillations during cross-polarisation (CP) has been made by Muller et al. in

Figure 3: (a) R.F. pulse diagram for the Hartmann-Hahn cross polarisation experiment. (b) Energy levels of two spins I and S in the static  $B_0$  field. (c) Energy levels in the presence of r.f. field during  $\tau$  are matched to enable polarisation transfer.



a single crystal of ferrocene [17]. In liquid crystals such as MBBA (Fig. 5),  $^{13}\text{C}$  spectra containing sharp well-resolved lines can be obtained by the use of the CP sequence (Fig. 4a). The intensities of the carbon lines show an oscillatory build-up when recorded as a function of the contact time  $t$  [20]. These oscillations are observed when the dipolar couplings of a carbon to its nearest neighbour protons are much stronger than the coupling of this spin system to the rest of the protons. The oscillation frequency  $f$  is given by

$$M_s = \frac{1}{2} M_{s0} (1 - \cos(ft)) \quad (1)$$

where  $M_{s0}$  and  $M_s$  are the peak value and the value at any time  $t$  respectively of the magnetization. The value of  $f$  is given in terms of  $D$ , the C–H dipolar coupling. It also depends on the number of equivalent protons coupled to a carbon. Thus for an IS spin system, such as a C–H group,  $f = D$  and for the  $I_2S$  spin system such as the  $\text{CH}_2$  group,  $f = \sqrt{2} D$ . For the methyl group ( $I_3S$  case), three values for  $f$  may be expected corresponding to  $D$ ,  $\sqrt{3} D$  and  $2D$ . Here the dipolar coupling  $D$  expressed in kHz is defined as

$$D = (-h\gamma_C\gamma_H/4\pi^2 r_{CH}^3) S_{CH} \quad (2)$$

where  $\gamma_H$ ,  $\gamma_C$  are the gyromagnetic ratios of the protons and carbons respectively,  $r_{CH}$  is the

internuclear vector and  $S_{CH}$  is the order parameter along the direction of this vector. The value of  $(h\gamma_C\gamma_H/4\pi^2 r_{CH}^3)$  is 22.68 kHz for  $r_{CH}$  1.1 Å. Equation (1) is further modified [17] to take into account spin diffusion between the protons directly coupled to the carbon under consideration and the rest of the protons in the system as

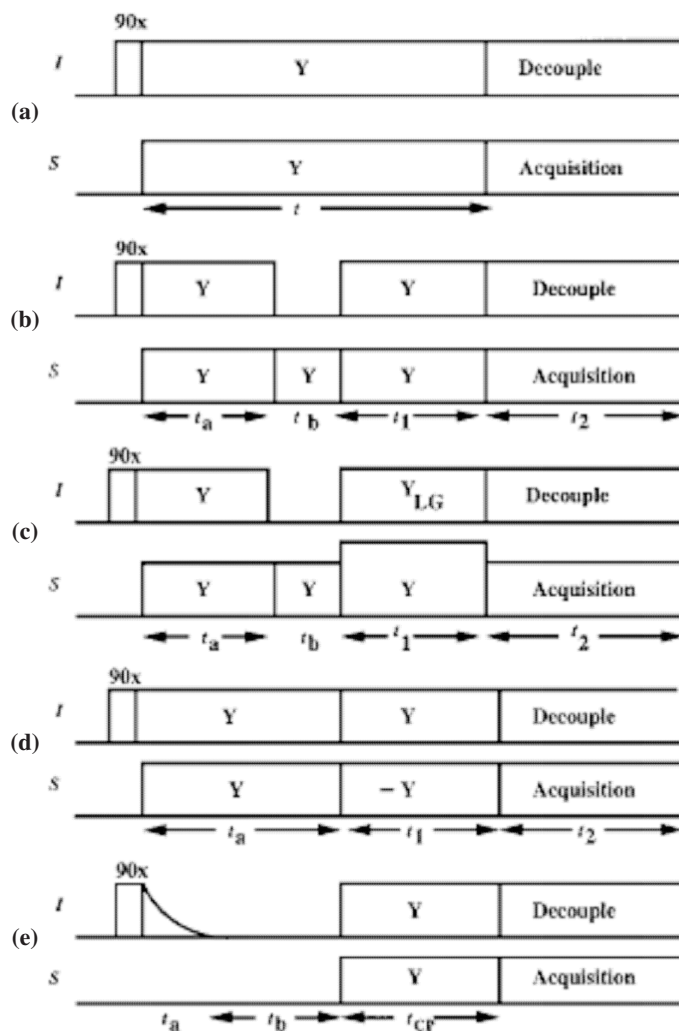
$$M_s = M_{s0} \left[ 1 - \frac{1}{2} \exp(-t/T_{II}) - \frac{1}{2} \exp(-3t/T_{II}) \cos(ft) \right] \quad (3)$$

where  $T_{II}$  represents the time constant for the spin diffusion process.

Fig. 5 shows the proton decoupled  $^{13}\text{C}$  spectrum of MBBA at room temperature. Fig. 6 presents the variation of the intensities of the  $C_7$ ,  $C_\alpha$ ,  $C_\beta$ , and  $C_\gamma$  carbons as a function of the contact time. The oscillation frequency  $f$  and hence dipolar coupling  $D$  can be obtained by fitting Eq. (3) to the experimental data. Values of 3.73, 4.84, 2.76, and 2.84 kHz were obtained for  $D$  respectively for the  $C_7$ ,  $C_\alpha$ ,  $C_\beta$ , and  $C_\gamma$  carbons of MBBA. The  $C_7$  dipolar coupling enables the order parameter  $S$  of the aromatic core to be estimated with the assumption of uniaxial ordering from

$$D = -S(h\gamma_C\gamma_H/4\pi^2 r_{CH}^3)(3\cos^2\theta - 1)/2 \quad (4)$$

Figure 4: Various cross-polarisation pulse schemes employed for obtaining dipolar couplings: (a) Hartmann–Hahn cross-polarisation, (b) cross-depolarisation, (c) cross-depolarisation with Lee–Goldburg decoupling, (d) polarisation inversion, (e) cross-polarisation from the dipolar bath.



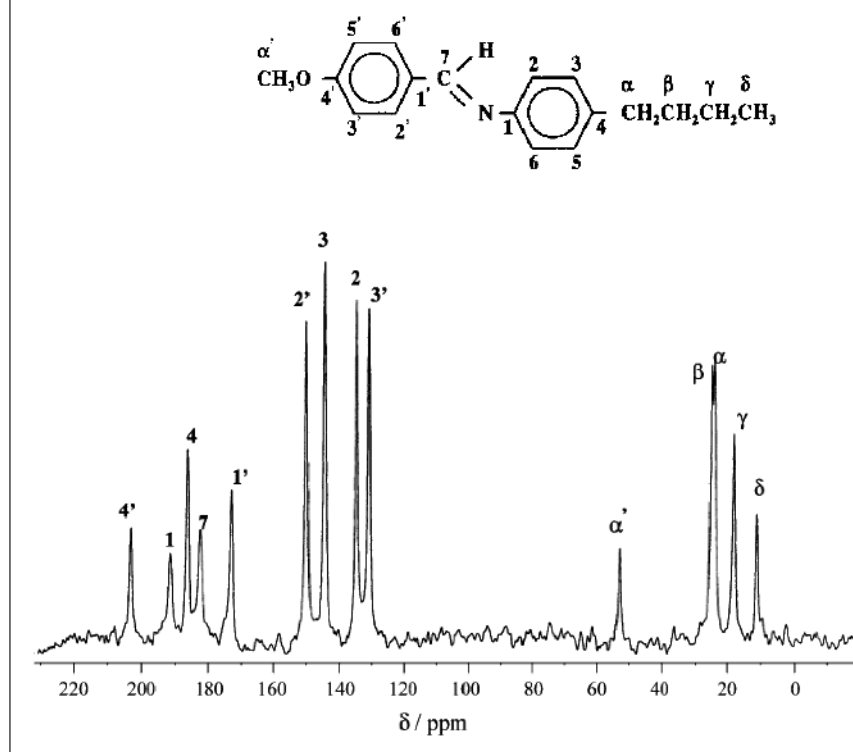
where  $\theta$  is the angle between the director and the C–H bond. Using a value of  $114^\circ$  for the C–C–H bond angle and assuming a tilt of the director by  $3.5^\circ$  from the para-axis of the adjacent phenyl ring a value of  $S = 0.52$  was obtained from these measurements, which agrees well with values reported by using other methods. The magnitude of the order parameter along the aliphatic chain averaged over several conformations can also be calculated from Eq. (2) using the obtained values of dipolar couplings. Values of 0.21, 0.12, and 0.13 obtained for the carbon sites  $\alpha$ ,  $\beta$  and  $\gamma$  are in agreement with the variation of order parameter generally observed in liquid crystalline systems.

A straightforward way of obtaining the oscillation frequencies is to use the 2D approach where the CP contact time ( $t$ ) is incremented in

regular steps between successive experiments. A two-dimensional data set is collected with proton decoupling during  $t_2$ . A two-dimensional Fourier transform then gives  $^{13}\text{C}$  chemical shifts along the  $F_2$  axis and the oscillation frequencies along  $F_1$ . A cross-depolarisation experiment (Fig. 4b), rather than a cross-polarisation experiment provides better results. The axial peaks which arise from the non-oscillatory terms of Eq. (3) is less intense in the former case. The S spin magnetization during the  $t_1$  period is given by

$$M_s = M_{so} \left[ \frac{1}{2} \exp(-t_1/T_{II}) + \frac{1}{2} \exp(-3t_1/T_{II}) \cos(ft_1) \right]. \quad (5)$$

Figure 5: Proton-decoupled  $^{13}\text{C}$  spectrum of the liquid crystal MBBA recorded on a Bruker DSX-300 NMR spectrometer at 75.47 MHz at room temperature.



The peaks along the  $F_1$  axis provide the oscillation frequencies  $f$  from which the dipolar couplings can be estimated using the prescription provided earlier. Results of such an experiment carried out with  $t_a = 1$  ms and  $t_b = 200$  ms are shown in Fig. 7 for the aliphatic carbons of MBBA. There are cross peaks occurring at 6.8, 3.8 and 4.0 kHz corresponding to the  $C_\alpha$ ,  $C_\beta$ , and  $C_\gamma$  carbons, which provide the corresponding C–H dipolar couplings as 4.8, 2.7, and 2.8 kHz.

### Inclusion of Homonuclear Decoupling during CP

The dipolar oscillations during CP are highly damped due to the couplings among the protons. Consequently the peaks in the two-dimensional spectra are broad and in several instances hard to observe. Wu et al. [30] have shown that the use of Lee–Goldburg (LG) decoupling [31] during cross-polarisation results in the removal of homonuclear dipolar couplings leading to a reduction of the line width along the dipolar axis. The use of the method has been made for the case of the liquid crystal N-(4-ethoxybenzylidene)-4-n-butylaniline (EBBA) [21]. The pulse sequence used for the 2D experiment is shown in Fig. 4c. The  $t_1$  period corresponds to exchange of polarisation

between carbons and protons. During this period the proton offset is changed to satisfy the Lee–Goldburg condition and carbon power level is adjusted to satisfy the Hartmann–Hahn condition so that magnetization exchange takes place under homonuclear proton spin decoupling. The effect of LG decoupling can be seen as a lengthening of the dipolar oscillations in comparison to the on-resonance spin-lock experiment. The homonuclear decoupling during the  $t_1$  period results in the scaling of the heteronuclear couplings, the theoretical scaling factor being  $\sin \theta_m = 0.82$ , where  $\theta_m$  is the magic angle. Using this pulse-scheme, the two-dimensional spectrum of EBBA was obtained at several temperatures and C–H dipolar couplings at several sites were measured. From the dipolar couplings of the benzylidene carbon, the order parameter of the aromatic core was obtained at these temperatures. Oscillation frequencies were obtained for the aromatic carbons also. From the values of order parameter of the core at different temperatures, the proton–carbon dipolar couplings of phenyl ring methine carbons can be calculated, assuming a hexagonal geometry of the phenyl ring and fast flip motion about the para axis. In this case, the one bond C–H dipolar coupling  $D_{CH}^1$  is nearly the same as the coupling of this carbon to

Figure 6: Relative intensities of signals of (a)  $C_\gamma$ , (b)  $C_{\alpha}$ , (c)  $C_{\beta}$ , and (d)  $C_\gamma$  carbons of MBBA obtained using the pulse sequence shown in fig.4a and plotted against contact time  $t$ . Points correspond to experimental values and the continuous line corresponds to the fit of the data to Eq. (3) with (a)  $f = 3.73$  kHz,  $T_{II} = 333$  ms, (b)  $f = 6.84$  kHz,  $T_{II} = 181$  ms, (c)  $f = 3.90$  kHz,  $T_{II} = 228$  ms, and (d)  $f = 4.0$  kHz,  $T_{II} = 273$  ms.

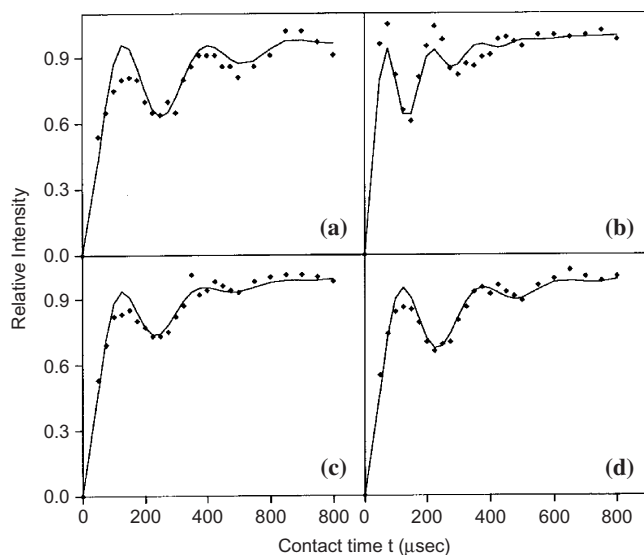
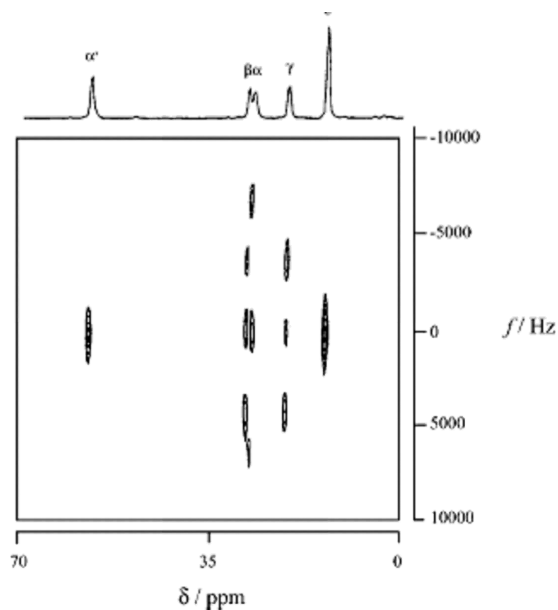


Figure 7: Two-dimensional spectrum of the aliphatic carbons of MBBA obtained using the pulse sequence shown in Fig. 4b on a Bruker DSX-300 NMR spectrometer at 75.47 MHz at room temperature. The horizontal axis corresponds to  $^{13}\text{C}$  chemical shifts and the vertical axis to the dipolar oscillation frequencies. The projection along the horizontal axis of the two-dimensional spectrum is also shown.



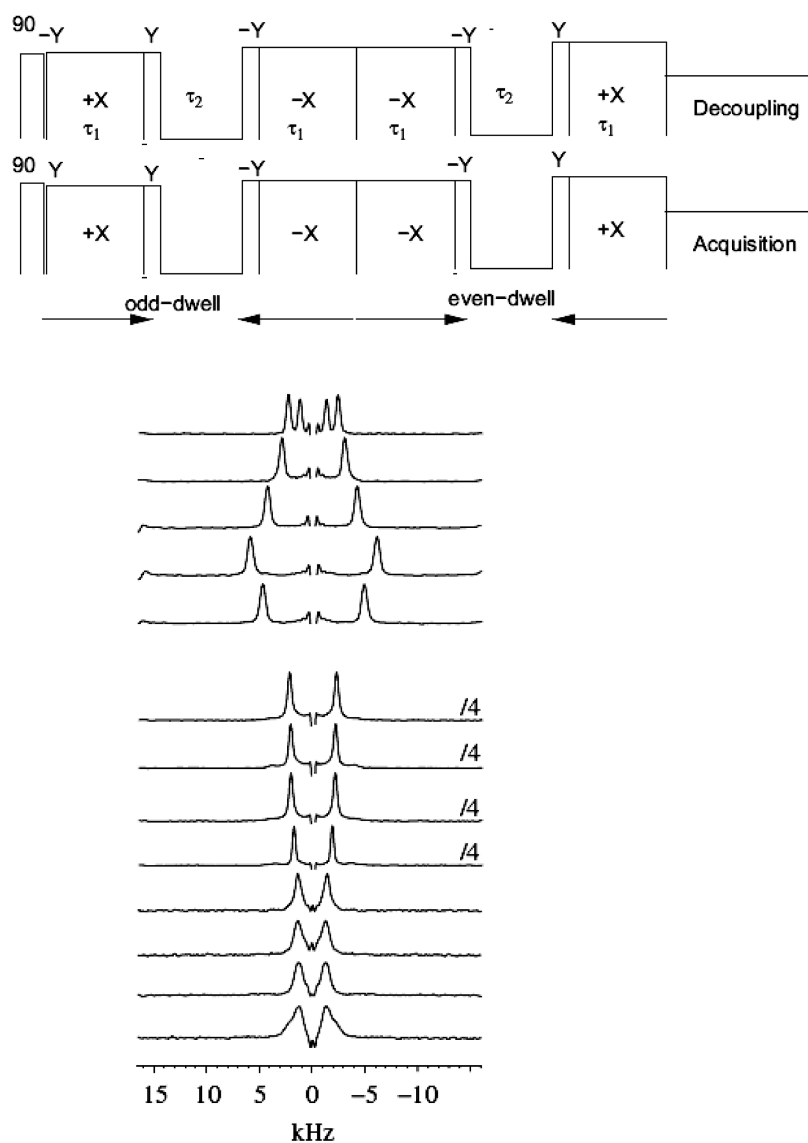
its ortho-proton  $D_{CH}^2$  due to the effect of ordering being different along different directions. In such cases, where the carbon is coupled to more than one proton, the evolution of magnetization is expected to proceed in a locked mode [18] and the oscillation frequency is given by  $[(D_{CH}^1)^2 + (D_{CH}^2)^2]^{1/2}$ . The values thus calculated and the experimental oscillation frequencies are observed to show a good correlation [21].

Experiments involving off-resonance irradiation such as the Lee–Goldburg decoupling are observed to be sensitive to proton carrier-frequency offsets and Hartmann–Hahn matching condition. Therefore sequences which are less prone to errors in the measurement of dipolar couplings arising out of above causes are being investigated. One of the pulse sequences proposed to solve the above problems uses the so-called “magic sandwich” pulses for removing proton–proton dipolar couplings (32). The scheme uses the fact that the secular part of the homonuclear dipolar interaction changes sign and reduces to half its value in the rotating frame. Therefore evolution under the homonuclear dipolar coupling undergoes a time-reversal when alternated between evolution in the laboratory frame and in the rotating frame and for appropriate evolution period the coupling averages to zero. However heteronuclear coupling is not averaged. Hence, by employing Hartmann–Hahn match, coherent polarisation transfer between I and S spins can be achieved and the dipolar coupling measured. This pulse scheme has further been improved incorporating the magic sandwich in the S spin also so that it removes homonuclear couplings among S spins [25]. It also incorporates  $90^\circ$  pulses on both I and S spins at the beginning of the sequence to enhance dipolar cross-peak intensities, which is discussed subsequently. The pulse sequence named as “EXE-MS2” and the results obtained on a liquid crystalline sample of 5CB are presented in fig. 8. Further modifications to the pulse scheme to reduce the r.f. power used and hence heating of the sample have also been reported (26). The use of on-resonance r.f. irradiation and suitable r.f. phase alternation in the above schemes renders these schemes more reliable for the measurement of the dipolar couplings.

### Enhancing Cross-peak Intensities

As pointed out earlier, Eq. (3) governs the frequencies and intensities of the peaks along the dipolar axis in the 2D experiments. The oscillatory cosine term gives rise to the cross peaks containing dipolar coupling information. There is also the non-oscillatory part which gives rise to the zero frequency peaks, which may overlap with cross peaks close to the center, causing difficulties in measuring

Figure 8: **Top:** 2D-Pulse sequence “EXE-MS2” that enables polarisation exchange between spins I and S with homonuclear dipolar decoupling for both nuclei. **Bottom:** Cross sections of the 2D spectrum showing the IS dipolar splittings for different carbons of the liquid crystal 5CB. The traces from top to bottom correspond to carbons labeled as (ref. Fig. 2)  $\omega$ ,  $\delta$ ,  $\beta$ ,  $\alpha$ ,  $\gamma$ , 2, 2', 3, 3', 4', 1, 1' and 4. Vertical scales for the cross-sections are indicated wherever they are different.

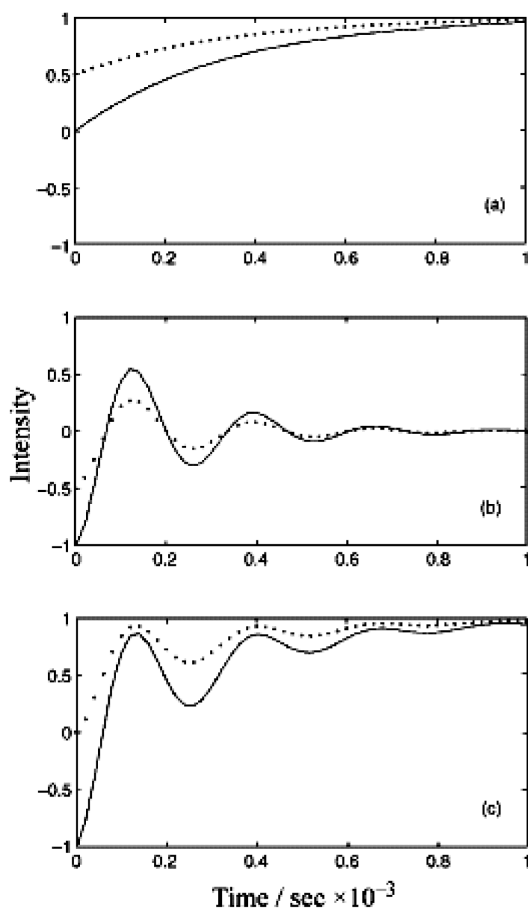


small dipolar couplings. For attenuating the zero frequency peaks, use of polarisation inversion instead of cross polarisation has been utilized [22, 30]. The polarisation transfer process for a two spin I-S system can be modeled as a coherent process in mutually commuting zero-quantum and double-quantum manifolds [33]. Under the assumption of high r.f. fields, the dipolar coupling causes as oscillatory evolution of the density matrix in the zero quantum frame, while in the double quantum frame the density matrix remains constant. The former gives rise to the cross peaks and the latter to

the axial peak. In polarisation inversion (Fig. 4d) there is an initial polarisation transfer from I spins to S spins during  $t_a$ . At the end of this period the two spin system can be taken to be completely polarised due to contact with the proton bath. Thus the initial density matrix  $I_z$  tends to become the double quantum density operator  $I_z + S_z$ . Inversion of the r.f. field for the S spin at this point corresponds to a change of sign of the S spin Hamiltonian or equivalently the density matrix can be thought of as equal to  $I_z - S_z$ , which is an operator in the zero quantum sub-space. As a result the initial



Figure 9: S spin magnetization evolution due to (a) double quantum (b) zero quantum processes, and (c) combined effect of results shown in (a) and (b) during polarisation (.....) and polarisation inversion (—). The plots correspond to values of  $f$  and  $T_{II}$  being 3.73 kHz and 333 ms.



evolution of magnetization during polarization inversion takes place only in the zero-quantum subspace. Therefore the dipolar cross-peaks are much more intense than the axial peaks enabling even small dipolar couplings to be observed. At larger contact times, the double-quantum evolution does come into play [22] and the equation governing this process is given by

$$M_s = M_{s0} [1 - \exp(-t_1/T_{II}) - \exp(-3t_1/T_{II}) \cos(ft_1)]. \quad (6)$$

Fig. 9 shows the contribution to the S spin intensity from the zero quantum and the double quantum evolution as well as the combined effect for both cross-polarisation and polarisation inversion experiments. It is observed that polarization inversion leads to a doubling of the amplitude of the oscillatory part and also to a reduction in the initial value of the non-oscillatory component. In a 2D

experiment, this would lead to a doubling of the cross-peak intensity and a significant reduction of the axial peak intensity.

In the scheme discussed above an extra period of r.f. irradiation in the form of the polarisation inversion has been added. This can contribute to unwanted sample heating. Therefore alternate means of enhancing cross-peak intensities, with the use of minimal r.f. power are being explored. A pulse-scheme suggested uses the polarisation of the S spin in the static magnetic field also, which otherwise is neglected (23,24). This scheme named as “EXE-CP” involves the application of a  $90^\circ$  degree pulse in the beginning of the CP period on the S spin along with the  $90^\circ$  pulse applied on the I spin. This causes a reduction in the axial peak intensity and enhances the cross-peak intensity by a factor of 67 % and is illustrated in fig. 10. Both simulation and experimental results for a sample of chloroform oriented in a liquid crystalline matrix have been presented.

#### Mis-Matched Hartmann–Hahn Condition – CP from the Dipolar Reservoir

In the studies reported so far, polarisation transfer has been considered between the Zeeman reservoirs of I and S spins under Hartmann–Hahn match. For a mismatch of the Hartmann–Hahn condition, an absorptive Lorentzian behavior for the S spin intensity has been predicted [33] with the width of the Lorentzian being related to the homonuclear dipolar coupling of the abundant spins. A similar study in which the initial magnetization is in the dipolar bath rather than in the I spin Zeeman bath has also been reported [34] and on the basis of the quasi-equilibrium theory a dispersive Lorentzian behaviour for the S spin intensity has been predicted. The above polarisation transfer process has been considered in detail by carrying out experimental measurements for a range of mismatch conditions by utilizing the pulse scheme shown in Fig. 4e [29]. Here, an ADRF pulse sequence on the I spins creates a dipolar order from the I spin Zeeman order during the period  $t_a$ . During  $t_{CP}$  a Hartmann–Hahn cross-polarisation pulse sequence is used, which results in the transfer of polarisation from the dipolar bath to the S spin Zeeman bath. As seen from Fig. 11, the transfer process has the characteristics that S spin intensity is zero for  $\omega_{1S} = \omega_{1I}$ , positive for  $\omega_{1S} > \omega_{1I}$  and negative for  $\omega_{1S} < \omega_{1I}$ , where  $\omega_{1S}$  and  $\omega_{1I}$  are the strengths of the spin-lock r.f. on the S and I spins respectively during the CP process. The S spin intensity plotted as a function of  $\Delta\omega = \omega_{1S} - \omega_{1I}$  can be shown to be given by

$$M_s = \beta\lambda^2 \Delta\omega / (\Delta\omega^2 + \lambda^2) \quad (7)$$

Figure 10: Pulse sequences and spectra corresponding to (A) CP and (B) EXE-CP experiments. Spectra on the left are simulated and those on the right are experimental.

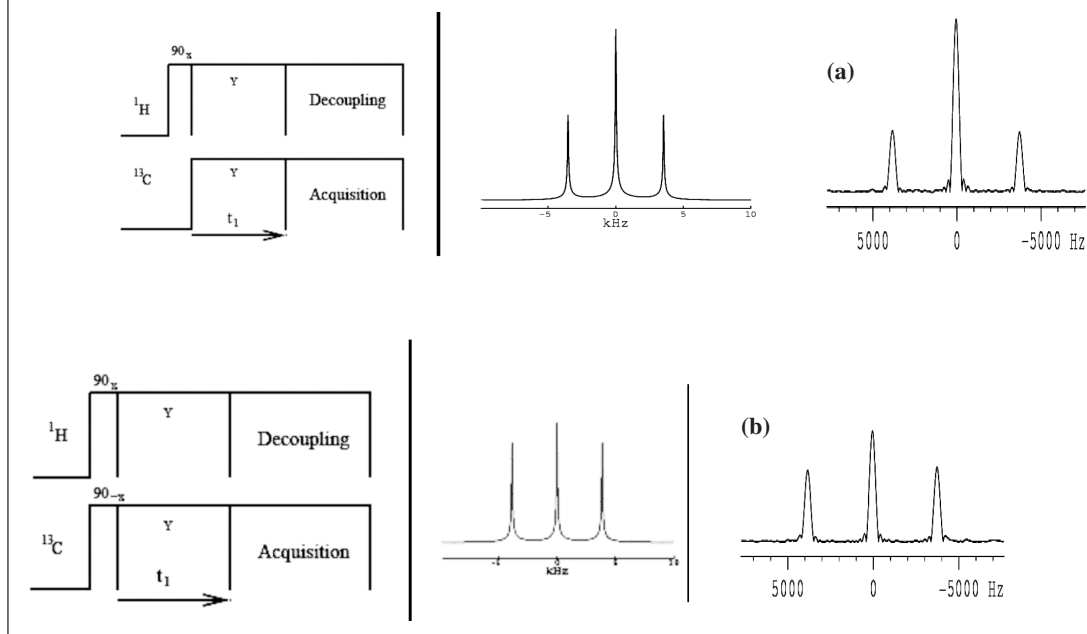
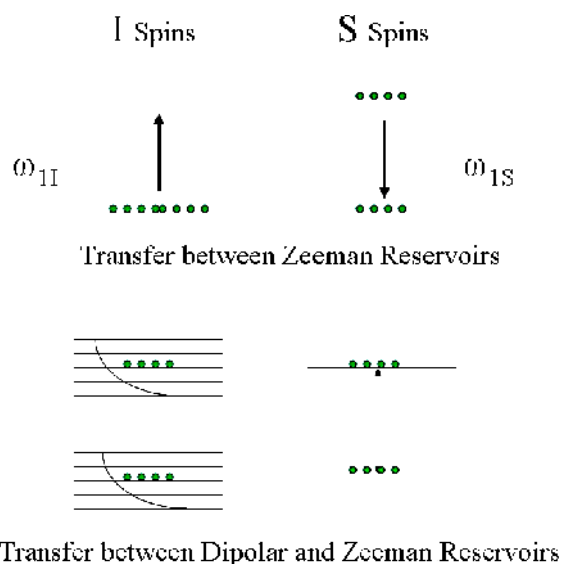


Figure 11: Nuclear spin population distribution. **Top:** Hartmann-Hahn CP. I-spin Zeeman states in the external magnetic field have a large population difference. **Bottom:** CP from the dipolar bath. I-spin population distributed in the quasi-continuum of dipolar energy states.

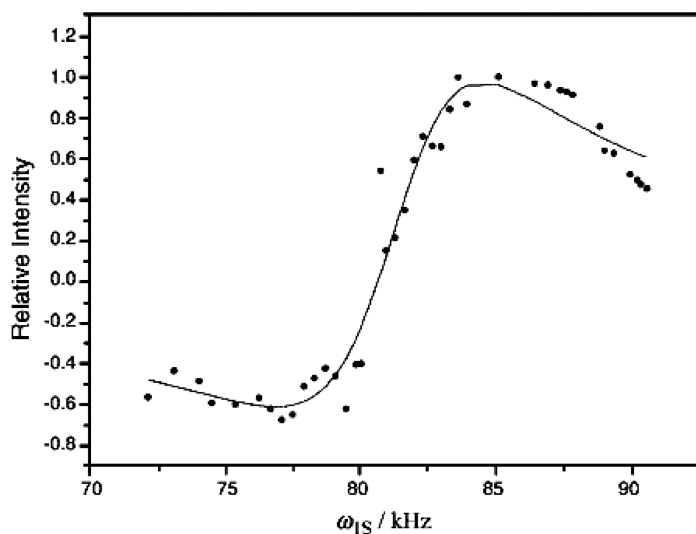


73

where  $\beta$  is the initial inverse spin temperature of the dipolar reservoir and  $\lambda^2$  is related to the I spin second moment. The experimental results for the carbon of EBBA in its oriented phase obtained

by observing the  $^{13}\text{C}$  resonance and by using the pulse sequence of Fig. 4e are shown in Fig. 12. The points correspond to the intensity of the carbon line as a function of  $\omega_{1S}$  for a fixed value of  $\omega_{1I}$ . It

Figure 12: Variation of cross-polarised signal intensity from the dipolar bath of protons to the  $\alpha$  carbons in the liquid crystal EBBA for different r.f. powers ( $\omega_{1S}$ ) on  $^{13}\text{C}$ . The experimental points have been obtained by using the pulse sequence of Fig. 4e, with  $t_a = t_b = 1$  ms and  $t_{CP} = 200\mu\text{sec}$ . The proton r.f. power ( $\omega_{1I}$ ) was kept constant at 83 kHz. The continuous curve corresponds to a fit of the experimental data to a mixture of dispersive and absorptive Lorentzian functions and yields a value of  $\lambda^2 = 14.2$  kHz $^2$  for the  $\alpha$  carbon



is observed that the plot indeed shows an overall dispersive Lorentzian behaviour. However, the fit of the data to Eq. (7) showed some deviations. A better fit to the experimental data could be obtained by including an additional absorptive Lorentzian of the same width which could arise due to transfer from remnant Zeeman magnetization of the I spins at the end of the ADRF period, cross polarizing directly to the S spins [29]. This continuous curve shown in Fig. 12 corresponds to the fit obtained using the above procedure. A value 14.2 kHz $^2$  for  $\lambda^2$  has been obtained for the  $\alpha$  carbon of EBBA. Other methylene carbons along the chain show a variation of  $\lambda^2$  that is expected on the basis of the variation of the local order parameters of the system. This method like the WISE technique [35], provides a means of indirectly monitoring proton dipolar couplings using the heteronuclear chemical shift dispersion.

#### DAPT- a New Method for Measurement of Dipolar Couplings

All of the methods mentioned above involved polarization exchange utilising Hartmann-Hahn match condition. This involved the use of magnetization spin-locked with r.f. fields for fairly long periods of time. This contributed to heating up the sample by the r.f. field and attended

instabilities and occasional loss of samples also. Setting up the required r.f. match condition is also not trivial, with mismatch giving rise to errors in the measurement of the dipolar coupling. Recently a method has been proposed for measuring dipolar couplings in oriented systems which does not need Hartmann-Hahn match (27,28). It involves evolution of the I spin magnetization under a homonuclear decoupling pulse sequence into two spin order terms such as  $2S_z I_x$  and subsequent conversion and refocusing into an  $S_y$  term. Such an evolution and the refocusing will occur due to the heteronuclear dipolar coupling between the two nuclei. The pulse sequence shown in Fig. 13 involves evolution of I spin under the BLEW-12 homonuclear decoupling pulse sequence (36) during the  $\tau_1$  period. A  $90^\circ$  pulse on the S spin creates the  $2S_x I_x$  term. During the  $\tau_2$  period an evolution under a phase shifted BLEW-12 irradiation converts this into  $S_y$  magnetization, which is then observed as the signal during the  $t_2$  period. Incrementing either  $\tau_1$  or  $\tau_2$  then provides an oscillatory signal whose Fourier transform provides the dipolar coupling. Such an oscillatory evolution for the  $^{13}\text{C}$  signal from chloroform oriented in a liquid crystalline medium is shown in Fig. 13.

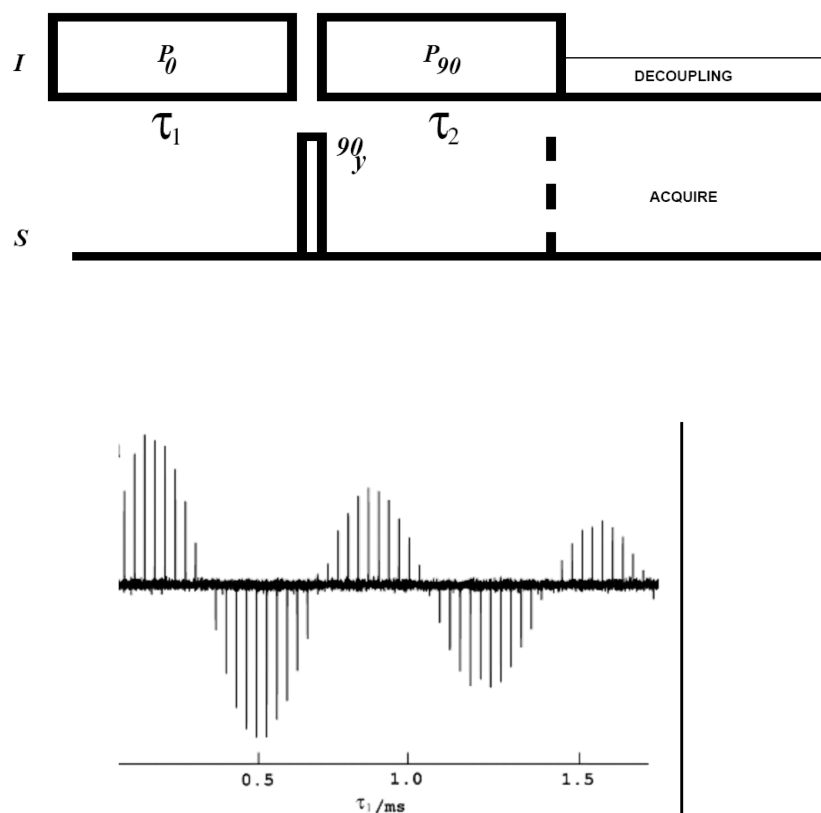
#### Applications

The cross-polarisation techniques mentioned above have been utilized to obtain dipolar couplings and order parameters in several novel liquid crystalline systems such as:

1. Aromatic systems containing four rings in the main core, a lateral hexyloxy chain, and a lateral aromatic branch with the aromatic ring itself being modified by different substituents at meta or para position [37].
2. Systems containing four rings in the main core, one terminal, and two nearby lateral chains on each of the outer aromatic rings [38].
3. Molecules containing the 2-phenylindazole core – the first bonds of the two terminal chains on the either side are not along the same axis due to the presence of the five membered ring in the core [39].
4. Systems containing three rings and a terminal hydroxyl group [40].
5. A thiophene-based three phenyl ring mesogen [41] and A mesogen consisting of a terminal dimethylamino group [42].

As an illustration of the use of the C–H bond order parameter obtained from utilizing the cross polarisation technique, systems containing three aromatic rings with a lateral crown-ether fragment and with oxyethylene (OE) units replacing the

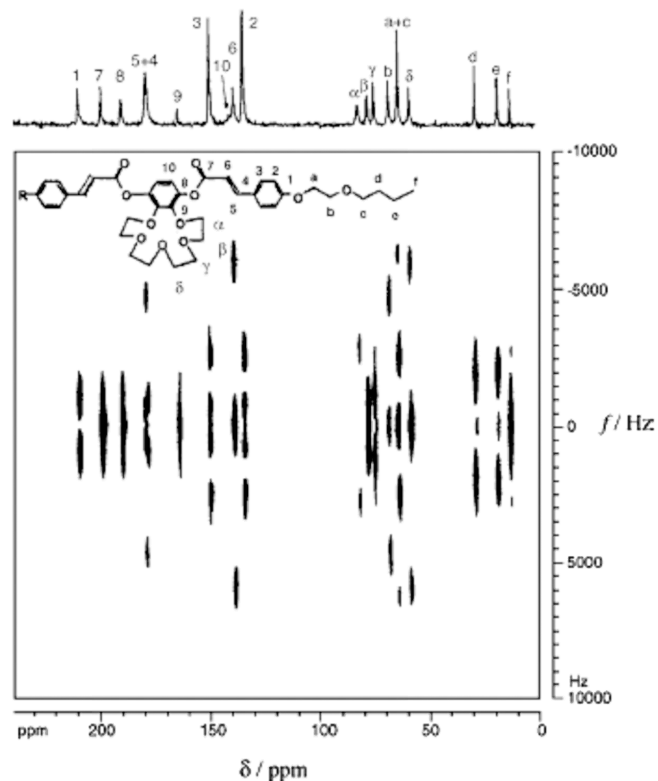
Figure 13: **Top:** DAPT pulse sequence.  $P_0$  and  $P_{90}$  denote blocks of BLEW-12 pulses applied during  $\tau_1$  and  $\tau_2$  respectively. Pulses applied during  $\tau_2$  have an additional phase shift of  $90^\circ$  compared to those applied during  $\tau_1$ . **Bottom:** The variation of intensity of the signal from chloroform oriented in the liquid crystal EBBA. The trajectory of the magnetization was followed by incrementing one BLEW-12 block at a time during  $\tau_1$ .



terminal alkoxy chains is presented [43] here. The replacement of the alkoxy chains by chains containing the oxyethylene units decreases the melting and clearing temperature so as to obtain nematic compounds near room temperature. The symmetric mesogen containing one OE unit in the terminal chain, referred to as CINPOE1Bu (Fig. 14) has been studied. The  $^{13}\text{C}$  chemical shifts in the isotropic phase and in the nematic phase at different temperatures have been monitored. The SLF 2D spectrum of the compound in its nematic phase at 349K obtained using the pulse sequence of Fig. 4d is shown in Fig. 14. From the peaks in dipolar dimension, the magnitudes of the dipolar interaction for several carbons have been obtained. For example, carbon  $C_a$  and  $C_c$  have the same chemical shifts, but have different dipolar couplings, the larger one being attributed to  $C_a$ , the first carbon in the terminal chain. In the crown-ether segment, it is noticed that the dipolar couplings decreases from  $C_\alpha$  to  $C_\gamma$ , but increases for  $C_\delta$ . This indicates that the average

angle between the C–H bond and the long molecular axis is less than the magic angle for carbons,  $C_\alpha$ , nearer to the magic angle for  $C_\beta$  and  $C_\gamma$  and greater than magic angle for  $C_\delta$ . This conclusion is supported by molecular modeling studies of the central part of a single molecule. For carbons in the polyoxyethylene chain, it is expected that the order parameter decreases monotonically with increasing distance from the core. This is in contrast to the odd–even effect usually observed in a terminal alkyl or alkoxy chain. Such a difference arises due to different probabilities for the conformers of the POE chain [44, 45]. In the system under consideration with one OE unit and one butyl fragment, the dipolar couplings decreases monotonically over the OE segment from carbon a to c while for the remainder of the carbons (d to f) the odd–even effect is present. The variation of the bond order parameter with temperature shows interesting correlation with the corresponding chemical shift of the carbon. A linear correlation between chemical shift and order parameter indicates that the conformation does

Figure 14:  $^{13}\text{C}$  SLF-2D spectrum of CINPOE1Bu, a liquid crystal containing a crown-ether and an oxyethylene unit in its nematic phase at 349 K, recorded on a Bruker DSX-300 NMR spectrometer at 75.47MHz.



not change significantly in the temperature range studied. Such a linear correlation has been observed for the carbons of the lateral crown ether. On the other hand, the non-linear correlation observed for the carbons of the OE unit indicates that the conformational probabilities change significantly with temperature resulting in different averaged values of the dipolar couplings and chemical shift anisotropies.

### Conclusions

NMR spectroscopy has been shown to be an extremely useful technique for the study of ordering and dynamics in liquid crystalline systems. Several parameters that can be extracted from the NMR experiments provide different means of obtaining such information. Particularly useful is the dipolar couplings between nuclei. The coherent effects of the cross-polarisation were shown to provide detailed information on dipolar couplings in nematic liquid crystalline systems. Various modifications and improvements to this experiment were also considered. The information thus obtained enables estimation of the order parameters of

the liquid crystals. Typical applications of the method were presented. In addition to the above studies where heteronuclear dipolar couplings were used, another cross-polarisation method that can provide information about the proton-proton dipolar couplings was also examined, thus providing another means of obtaining local order.

Received 18 March 2009.

### References

- Diehl P, Khetrapal CL (1969) NMR: Basic Principles and Progress 1: 1
- Emsley JW, Lindon JC (1975): NMR Spectroscopy using Liquid Crystal Solvents, Pergamon Press, Oxford
- Dong RY (1994) Nuclear Magnetic Resonance of Liquid Crystals, Springer, New York; (2004) Ann Rep NMR Spectrosc 53:67
- Spence R.D., Moses H.A and Jain P.C. (1953) J. Chem. Phys., 21: 380.
- Spence R.D., Gutowsky H.S. and Holm C.H. (1953) J. Chem. Phys. 21: 1891
- Emsley J.W. (Ed.) (1985), Nuclear Magnetic Resonance of Liquid Crystals, Reidel, Dordrech.
- Dong RY (1996) Encyclopedia of NMR, Grant DM, Harris RK, Wiley, Chichester, p2752; (2002) Prog Nucl Magn Reson Spectrosc 41:115
- Hoheney A, Muller A, Ernst RR (1979) Mol Phys 38: 909
- Fung B.M. (2002) Prog Nucl Magn Reson Spectrosc 41:171
- Magnuson ML, Tanner LE, Fung BM (1994) Liq Cryst 16: 857
- Magnuson ML, Fung BM, Schadt M (1995) Liq Cryst 19: 333
- Courtieu J, Bayle JP, Fung BM (1994) Prog Nucl Magn Reson Spectrosc 26: 141
- Fung BM (1996) Encyclopedia of NMR 4: 2744
- Caldarelli S, Hong M, Emsley L, Pines A (1996) J Phys Chem 100: 18696
- Hong M, Pines A, Caldarelli S (1996) J Phys Chem 100: 14815
- Caldarelli S, Lesage A, Emsley L (1996) J Am Chem Soc 118: 12224
- Muller L, Anil Kumar, Baumann T, Ernst RR (1974) Phys Rev Lett 32: 1402
- Hester RK, Ackerman JL, Cross VR, Waugh JS (1975) Phys Rev Lett 34: 993
- Hartmann SR, Hahn EL (1962) Phys Rev 128: 2042
- Pratima R, Ramanathan KV (1996) J Magn Reson A118: 7
- Nagaraja CS, Ramanathan KV (1999) Liq Cryst 26: 17
- Neeraj Sinha, Ramanathan KV (2000) Chem Phys Lett 332: 125
- Das BB, Ajithkumar TG, Ramanathan KV (2006) Chem. Phys. Lett., 426, 422
- Das BB, Ajithkumar TG, Sinha N, Opella SJ, Ramanathan KV (2007) J Magn Reson 185: 308
- Das BB, Ajithkumar TG, Ramanathan KV (2008) Solid State Nucl Magn Reson 33:57
- Das BB, Sinha N, Ramanathan KV (2008) J Magn Reson 194: 237
- Jayanthi S, Madhu PK, Kurur ND, Ramanathan KV (2007) Chem Phys Lett, 439: 407
- Jayanthi S, Madhu PK, Ramanathan KV (2008) J Phys Chem A112: 11159
- Venkatraman TN, Neeraj Sinha, Ramanathan KV (2002) J Magn Reson 157: 137
- Wu C, Ramamoorthy A, Opella SJ (1994) J Magn Reson A109: 270
- Lee M, Goldburg WI (1965) Phys Rev A140: 1261
- Nevzorov AA, Opella SJ (2005) J Magn Reson 185: 59
- Levitt MH, Suter D, Ernst RR (1986) J Chem Phys 84: 4243
- Zhang S, Stejskal EO, Fornes RE, Wu X (1993) J Magn Reson A104: 177

35. Schmidt-Rohr K, Clauss J, Spiess HW (1992) *Macromolecules* 25: 3273
36. Burum DP, Linder M, Ernst RR (1981) *J Magn Reson* 44: 173
37. Berdague P, Bayle JP, Fujimori H, Miyajima S (1998) *New J Chem* 1005
38. Berdague P, Munier M, Judeinstein P, Bayle JP, Nagaraja CS, Ramanathan KV (1999), *Liq Cryst* 26: 211
39. Berdague P, Judeinstein P, Bayle JP, Nagaraja CS, Neeraj Sinha, Ramanathan KV (2001), *Liq Cryst* 28: 197
40. Kalaivani S, Sakunthala PV, Narasimhaswamy T, Das BB, Ramanathan KV (Article Submitted)
41. Narasimhaswamy T, Lee DK, Somanathan N, Ramamoorthy A (2005) *Chem Mater* 17: 4567
42. Narasimhaswamy T, Monette M, Lee DK, Ramamoorthy A (2005) *J Phys Chem* 109: 19696
43. Neeraj Sinha, Ramanathan KV, Berdague P, Judeinstein P, Bayle JP (2002) *Liq Cryst* 29: 449
44. Rayssac V, Judeinstein P, Bayle JP, Kuwahara D, Ogata H, Miyajima S (1998) *Liq Cryst* 25: 427
45. Samulski ET, Dong RY (1982) *J Chem Phys* 77: 5090



**K. V. Ramanathan** received his PhD degree in Physics in 1978 from the Indian Institute of Science, Bangalore for his work on the development of the high pressure-low temperature wide-line NMR technique for the study of solids and the study of tunneling and ammonium ion dynamics. In 1977 he joined the Bangalore NMR Facility which eventually became a part of the Indian Institute of Science and switched to working on liquid state NMR and the development of two-dimensional NMR techniques. Subsequently he also became interested in the study of oriented systems and the application of the high-resolution solid state NMR methodologies such as cross-polarisation and magic angle/off-magic angle spinning to liquid crystals. His other interests include the study of quadrupolar systems and overtone spectroscopy and NMR applications to biological systems. Ramanathan has held various positions at the Indian Institute of Science. Currently he is a Professor and the Chairman of the NMR Research Centre at IISc. He is a Fellow of the National Academy of Sciences, India and a past President of the National Magnetic Resonance Society.